THE JOURNAL OF PHYSICAL CHEMISTRY C

C: Energy Conversion and Storage; Energy and Charge Transport

Coexistence of MLCT Excited States of Different Symmetry upon Photoexcitation of a Single Molecular Species

Paola Soledad Oviedo, German Eduardo Pieslinger, Luis M. Baraldo, Alejandro Cadranel, and Dirk M. Guldi

J. Phys. Chem. C, **Just Accepted Manuscript** • DOI: 10.1021/acs.jpcc.8b09499 • Publication Date (Web): 09 Jan 2019

Coexistence of MLCT Excited States of Different Symmetry Upon Photoexcitation of a Single Molecular Species.

Paola S. Oviedo[a,b], German E. Pieslinger[a,b], Luis M. Baraldo[a,b], Alejandro Cadranel[a,b,c,*], Dirk M. Guldi.[c,*]

[a] Universidad de Buenos Aires, Facultad de Ciencias Exactas y Naturales, Departamento de Química Inorgánica, Analítica y Química Física, Pabellón 2, Ciudad Universitaria, C1428EHA, Buenos Aires, Argentina.

[b] CONICET – Universidad de Buenos Aires. Instituto de Química-Física de Materiales, Ambientes y Energía (INQUIMAE), Pabellón 2, Ciudad Universitaria, C1428EHA Buenos Aires, Argentina

[c] Department of Chemistry and Pharmacy & Interdisciplinary Center for Molecular Materials (ICMM), Friedrich-Alexander-Universität Erlangen-Nürnberg, Egerlandstr. 3, 91058 Erlangen, Germany.

Supporting Information Placeholder

ABSTRACT: Photoexcitation of [Ru(tpy)(bpy)(μ-CN)Ru(py)$_4$Cl]$^{2+}$ ([RuRu]$^{2+}$) at 387 nm results in the population of two ^{3}MLCT excited states of different symmetry that coexist in the nanosecond scale. Common to both states is an excited electron in a tpy-based orbital. Their configuration differs in the position of the hole. In one excited state, **^{3}MLCTz**, the hole sits in an orbital parallel to the intermetallic axis allowing for a strong metal-metal electronic interaction. As a result, **^{3}MLCTz** is highly delocalized over both metal centres and shows an intense photoinduced intervalence charge transfer (PIIVCT) NIR signature. In the other excited state, **^{3}MLCTxy**, the hole is localized in an orbital perpendicular to the intermetallic axis and hence, significant intermetallic coupling is absent. This state shows no PIIVCT in the NIR and its spectrum is very similar to the one observed for the monometallic [Ru(tpy)(bpy)(CN)]$^+$ reference. Both ^{3}MLCT excited states have nanosecond lifetimes. The intervening energy barrier for a hole reconfiguration between the two different ^{3}MLCT excited states offers the opportunity to exploit wavefunctions of different symmetry before either the interconversion between them or the decay to the ground state is operative.

INTRODUCTION

Photoinduced physicochemical phenomena are essential to those processes that made life on Earth possible. Photosynthesis of cyanobacteria, for example, produced atmospheric oxygen, while more advanced organisms started to build up the biomass on our planet through sunlight-powered biosynthesis. Photosynthesis is the prototype of energy-conversion. Nowadays, the scientific community regards it as a blueprint[1–3] to meet, for example, the UN sustainability goal of clean and affordable energy for mankind. By virtue of its abundance on earth's surface, sunlight drives photosynthetic reaction center models, photovoltaic or photoelectrochemical devices, photo-magnets, photo-triggered molecular machines, etc.[4] Undoubtedly, the needs for a sound understanding of and control over photoinduced phenomena, through the development of simple models, remains a tremendous challenge.

Multimetallic coordination compounds constitute a versatile platform for developing architectures that convert energy. A careful design strategy includes, on one hand, the individual fine-tuning of the physicochemical properties of monometallic complexes and, on the other hand, their synergetic assembling through coordinative interactions. Leading examples are chromophore-catalyst assemblies, which, for example, mimic the photosynthetic antenna complexes and reaction centers,[5–7] or multi chromophore associates, which behave as molecular antennae.[8,9] Usual strategies are based on the use of metal ions and ligands as electron donors and acceptors, respectively, enabling MLCT absorptions throughout the visible range. As a matter of fact, they act as antennae and funnels of energy or charges to reach the catalytic sites or electrodes.

Considering the chemical stability and electrochemical and photophysical suitability of bimetallic {M-M'} fragments bearing Ru(II), Os(II), Ir(III), Re(I) and Rh(III), they have emerged as models for chromophore-catalyst assemblies and molecular antennae.[10–20] In the excited state, these systems can present unique electronic configurations that are impossible in monometallic complexes. For example, a metal to ligand charge transfer in one of the fragments results in a mixed valence system with a $(\pi^*_L)^1(d\pi_M)^5(d\pi_{M'})^6$ configuration that bears a ligand-centered radical anion in one of the coordination spheres.[21]

There is an extensive literature of mixed-valence complexes in the ground state, especially for systems with a $(d\pi_M)^5(d\pi_{M'})^6$ electronic configuration. These are simple models for studies on metal-metal electronic communication, which is of great relevance in the context of energy conversion.[22–28] The position, intensity, and shape of their intervalence charge transfer (IVCT) transitions enables insights into those physicochemical parameters that relate to the electron

transfer processes between the two metal centers.[29,30] Reports of *excited-state* mixed-valence species are rather scarce,[31–40] probably due the experimental challenge of detecting them. If both centers are sufficiently coupled, the resulting photoinduced mixed-valence (PIMV) state should give rise to a very distinctive strong photoinduced intervalence charge transfer (PIIVCT) absorption band in the NIR region, and hence should be detectable thanks to advances in detection systems and pump-probe setups.

Active engagement of delocalized mixed-valence excited states in the deactivation cascade of [Ru(tpy)(bpy)(μ-CN)Ru(py)$_4$Cl]$^{2+}$ ([RuRu]$^{2+}$) was recently postulated.[41] In this contribution we demonstrate that, upon photoexcitation of [RuRu]$^{2+}$, two excited states coexist in the nanosecond timescale. Femto/nanosecond NIR transient absorption techniques reveal the presence of PIIVCT bands that we assign to the photogenerated mixed valence species. Target analyses show that this excited state coexists on the nanosecond timescale with another state that lacks such a spectroscopic NIR feature. Our results illustrate that the added complexity of multimetallic systems could result in the presence of excited states with configurations of different symmetries, but similar low energies. As these excited states could have diverse reactivity and they could be addressed with different stimuli, it should be possible to use these multimetallic complexes as the basis of systems with controllable photoreactivity.

RESULTS AND DISCUSSION

The UV–vis-NIR absorption spectra of [RuRu]$^{2+}$ in acetonitrile at room temperature and the corresponding one-electron oxidized [RuRu]$^{3+}$ are presented in Figure 1.[41] Please note the broad absorption of moderate intensity for [RuRu]$^{3+}$ in the NIR region at 10400 cm^{-1} (960 nm, ε = 4350 M^{-1} cm^{-1}), which we assign to a ground-state intervalence charge transfer (GSIVCT) transition. [RuRu]$^{3+}$ is a non-symmetric Class II, ground-state mixed-valence (GSMV) complex where the hole is centered mainly in the {Ru(py)$_4$Cl} fragment. This is evidenced by the disappearance of the 10400 cm^{-1} band upon further oxidation (Figure S1)[29,42] (TD)DFT calculated electronic transitions are in sound agreement with the experimental spectra for both oxidation states (Figure S2 and Tables S1 and S2), including the GSIVCT for [RuRu]$^{3+}$, as it has been shown to occur in related systems.[43] The calculated spin density distribution also locates the hole on the {Ru(py)$_4$Cl} fragment (Figure S2).

[RuRu]$^{2+}$ reveals weak room temperature photoluminescence in argon-saturated DMSO. We explored the photoluminescence upon selective excitation of either {Ru(tpy)(bpy)} or {Ru(py)$_4$} at 19800 cm^{-1} (505 nm) or 25800 cm^{-1} (387 nm), respectively.[41] Regardless of the excitation energy, the emission maxima are always centered at 14400 cm^{-1} (695 nm) (Figure S3). The quantum yield under 505 nm illumination is ϕ_{505nm} = 1 x 10^{-3} and is comparable to that of analogous ruthenium polypyridines.[44] Upon 387 nm excitation, the photoluminescence quantum yields decrease to ϕ_{387nm} = 9 x 10^{-5} probably due to thermal population of low-lying *dd*-states (Table S3). Overall, our results match those obtained previously.[41]

Considering that the transient absorption results (vide infra) suggest the presence of more than one excited state on the nanosecond time scale, the photoluminescence lifetimes were reevaluated under 505 nm and 410 nm excitation, and treated with one-, two-, and three-exponential fitting functions (Figure S5). The best fits were based on biexponential fitting functions with $\tau_{pl}(1)$ = 1.3 ns and $\tau_{pl}(2)$ = 6.4 ns.[45] As $\tau_{pl}(1)$ and $\tau_{pl}(2)$ lack any meaningful dependence on the excitation wavelengths, we conclude that the same two photoluminescent states are, on one hand, populated on the nanosecond timescale and, on the other hand, independent on which center is initially photoexcited. Unfortunately, we could not spectrally resolve these emitting states even at 77 K, conditions in which [RuRu]$^{2+}$ emits at 674 nm (Figure S4).

The monometallic reference [Ru(tpy)(bpy)(CN)]$^{+}$ emits in DMSO at 14200 cm^{-1} (705 nm), independently of the excitation energy, with quantum yields of ϕ_{505nm} = 2.7 x 10^{-4} and ϕ_{387nm} = 2.8 x 10^{-4} and monoexponential lifetimes of τ_{505nm} = 13.4 ns and τ_{410nm} = 12.2 (Figure S3, Table S3). Notably, the low temperature emission of [Ru(tpy)(bpy)(CN)]$^{+}$ occurs at 643 nm, with a very similar bandshape in comparison with [RuRu]$^{2+}$ (Figure S4).

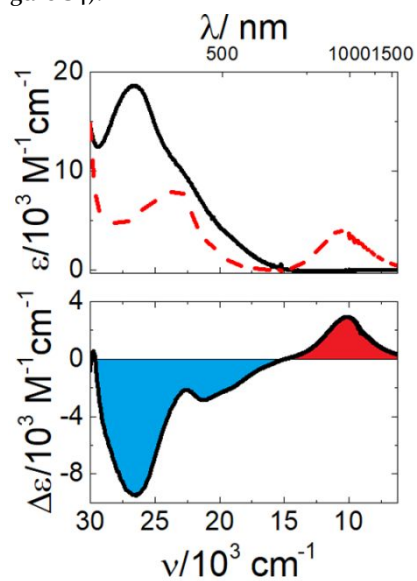

Figure 1. Top: UV-vis-NIR absorption spectra of [RuRu]$^{2+}$ (solid line) and [RuRu]$^{3+}$ (dashed line) in acetonitrile at room temperature. Bottom: Differential absorption spectrum upon oxidation.

To shed light on the nature of the photoluminescent states, vis-NIR transient absorption measurements with argon-saturated DMSO solutions of [RuRu]$^{2+}$ were performed on the nano-to-microsecond timescale upon 387 and 505 nm photoexcitation. Figures 2 and S7 show the differential absorption spectra at several delay times for 387 and 505 nm excitation, respectively. In Figure 2, the differential absorption spectrum at a 1 ns delay time reveals the presence of a very intense photoinduced absorption in the NIR at 6900 cm^{-1} (1450 nm). The lack of a similar transition for the corresponding [Ru(tpy)(bpy)(CN)]$^{+}$ monomer (Figure S8) leads us to the assignment of this band in the differential spectrum of ([RuRu]$^{2+}$)* as a PIIVCT transition. The observation of this

band implies that the hole corresponds to a dπ orbital that is mixed with the π orbitals from the cyanide bridge and those of the second metallic center, i.e. d_{xz} or d_{yz} (with z the main axis of the molecule). This excited state is therefore labeled as **³MLCTz**. The shape and properties of the PIIVCT (vide infra) suggest that in this excited state the hole is delocalized over the bimetallic complex, hence its configuration is $\{Ru^{II/III}(tpy^{-})(bpy)(\mu\text{-}CN)Ru^{II/III}(py)_4Cl\}$.

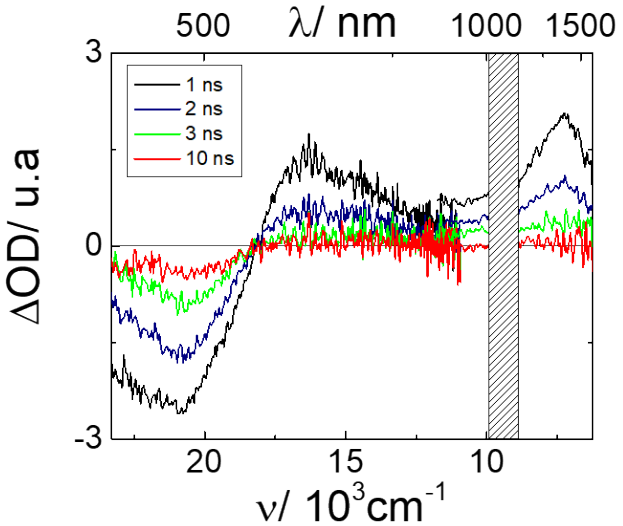

Figure 2. Selected differential absorption spectra of $[RuRu]^{2+}$ at delay times of 1 ns (black line), 2 ns (blue line), 3 ns (green line), and 10 ns (red line) in DMSO following excitation at 387 nm.

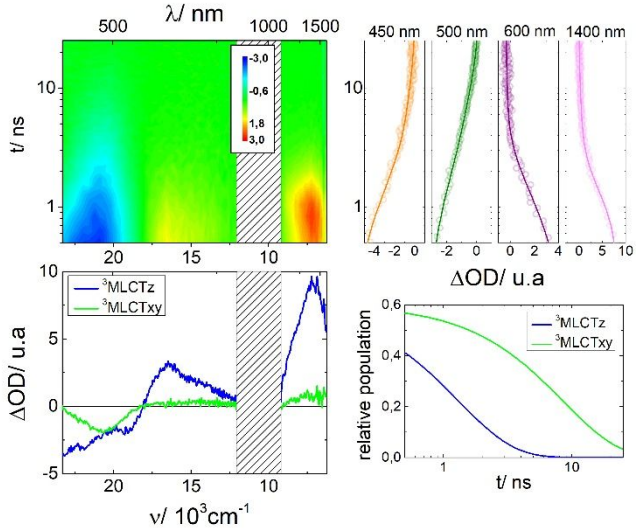

Figure 3. Upper left: Differential absorption 3D map obtained from nanosecond pump-probe experiments (λ_{exc}= 387 nm) for $[RuRu]^{2+}$ in DMSO at room temperature. Upper right: Time absorption profiles (open circles) and corresponding fittings from target analysis (solid lines) using a parallel two-state model. Bottom left: Species-associated differential spectra of **³MLCTz** (blue line) and **³MLCTxy** (green line) for $[RuRu]^{2+}$ upon excitation at 387 nm. Bottom right: Concentration evolution over time.

At 3 ns (Figure 2, Figure S7 for 505 nm excitation), the PIIVCT signature is absent, while other signals are still discernable: a bleaching centered at 20600 cm⁻¹ (485 nm) as well as a broad, but weaker photoinduced absorption at < 18200 cm⁻¹ (λ > 550 nm). In other words, an excited state different from **³MLCTz** is also present. Notably, the differential absorption spectrum at this time delay is very similar to that observed for the $[Ru(tpy)(bpy)(CN)]^{+}$ reference (Figure S8), where the negative signal mirrors ground state absorption, and the broad and weak positive signal is mainly due to radical anion ligand centered π* ← π* photoinduced absorptions. Therefore, we assign it to a ³MLCT excited state localized on {Ru(tpy)(bpy)}, where the electron is also located in the tpy ligand while the hole is in d_{xy}, an orbital pointing towards the radical anion and perpendicular to the bridge, i.e. $\{Ru^{III}(tpy^{-})(bpy)(\mu\text{-}CN)Ru(py)_4Cl\}$ or **³MLCTxy**.

The decay of the PIIVCT signal does, however, not coincide with the growth of the **³MLCTxy** bleaching. This led us to postulate that both species coexist and we performed target analyses to test the simultaneous presence of two species. By fitting the decay data with two species, we obtained lifetimes of 1.3 and 6.3 ns and spectra that are shown in Figure 3 (Figure S9 for 505 nm excitation, Tables S4 and S5).[46] Both lifetimes are in sound agreement with those obtained by TCSPC. Overall, these lifetimes are shorter than those usually observed for {Ru(tpy)(bpy)}-based ³MLCTs.[44,47,48]

The differential absorption spectrum of **³MLCTz** is similar to that obtained from the one-electron oxidation of $[RuRu]^{2+}$ (Figure 1). This suggests that a common mixed valence configuration of the hole exists for both the photo- and electrogenerated state. At this point, it is, however, important to note the differences between the GSIVCT signature of $[RuRu]^{3+}$ (Figure 1) and the PIIVCT signature of **³MLCTz** (Figure 3). In the ground state, the energy difference between the redox potentials for the oxidation of the ruthenium centres is 0.87 V.[41] This results in a GSIVCT signature at 10400 cm⁻¹ in acetonitrile. The PIIVCT is, however, seen at 6900 cm⁻¹ and correspondingly suggests a much smaller energy gap between the metallic dπ orbitals. We ascribe this red-shift to the presence of the tpy^{-} radical anion as part of the ³MLCT excited state. It destabilizes the ruthenium orbitals in {Ru(tpy)(bpy)} and brings them closer in energy to those of $\{Ru(py)_4Cl\}$. The direct consequence of this shift is a more even distribution of charges in **³MLCTz** than in the GSMV state. A similar reasoning has been used in conjunction with the shifted photoinduced LMCT markers, in comparison with GS LMCT absorptions, in, for example, {Ru(NCS)} complexes.[49] Notably, this is one of the very few examples in the literature, where a PIIVCT signal is reported.[31–40]

Our PIIVCT assignment of the NIR photoinduced transition in **³MLCTz** spectrum was independently supported by theoretical calculations. DFT methods were employed to identify the lowest triplet excited state of $[RuRu]^{2+}$ and its electronic configuration and (TD)DFT calculations were performed to simulate its electronic spectra. Notably, the calculated spectrum presents a NIR electronic transition at 6900 cm⁻¹ (Table S6, Figures S10 and S12), which is in sound agreement with that observed experimentally (Figure S12). Hence, the calculated electronic distribution is a very good approximation to that of **³MLCTz**. A plot of the spin density

for the calculated lowest triplet excited state (Figure S12) shows that the hole sits in a delocalized orbital, which is parallel to the intermetallic axis. Moreover, Mulliken spin densities of 0.50 and 0.47 for the metal ions in {Ru(tpy)(bpy)} and {Ru(py)$_4$}, respectively, are obtained (Figure S12). However, it should be considered that DFT methods tend to miscalculate the energy of delocalized configurations,[50,51] due the so-called "self-interaction error" that involves the residual interaction of an electron with itself.[52,53] Therefore, the conclusion that **^{3}MLCTz** is the lowest triplet excited state, especially in comparison with other low energy excited state as **^{3}MLCTxy**, is not valid

The differences in the NIR spectral region between **^{3}MLCTz** and **^{3}MLCTxy** relate to the symmetry of their configuration. In **^{3}MLCTz**, the hole sits in orbitals parallel to the intermetallic axis and, in turn, allows for mixing between both metallic centres and the cyanide bridge. Both a high degree of hole delocalization and the presence of the intense PIIVCT absorption stem from the electronic coupling in **^{3}MLCTz**. In fact, the asymmetric shape of the PIIVCT band compares well with previous observations for IVCTs in delocalized cyanide bridged systems (Figure S13) and suggest that **^{3}MLCTz** is an excited-state Class III mixed valence complex.[54] Moreover, the energy and shape of this transition show no significant differences in different solvents (Figure S14). The lack of dependence on the nature of the solvent of properties of the IVCT transitions is a common marker to identify a Class III mixed-valence complex.[21,29]

For **^{3}MLCTxy,** the absence of intense absorptions in the NIR leads us to propose an electronic configuration where the hole is placed into an orbital perpendicular to the intermetallic axis, precluding strong interactions between the metal centers.[55,56] Therefore, in **^{3}MLCTxy** the hole is mostly localized on {Ru(tpy)(bpy)}. These observations resemble those seen for ground-state mixed-valence [Ru(T)(bpy)(μ-NC)Ru(py)$_4$(CN)]$^{3+}$ and [Ru(T)(bpy)(μ-NC)Ru(MeOpy)$_4$(CN)]$^{3+}$ (T = tpy or tris(1-pyrazolyl)methane). There, the symmetry of the (GS)HOMOs is modulated by pyridine substitution.[57] In the earlier case, the (GS)HOMO is parallel to the intermetallic axis and, in turn, delocalized. The outcome is a strong GSIVCT absorption. In the latter case, the (GS)HOMO is perpendicular to the intermetallic axis and localized on {Ru(MeOpy)$_4$}, yielding much weaker GSICVTs. In [RuRu]$^{2+}$, the different electronic configurations are, however, not a direct consequence of a different substitution; instead the two coexist upon photoexcitation.

To unveil the excited-state dynamics that create the aforementioned excited state scenario, we turned to picosecond vis-NIR transient absorption measurements with argon-saturated DMSO solutions of [RuRu]$^{2+}$ under 387 nm photoexcitation (Figure 4). Global analyses of the data result in four sequential decays with lifetimes of 12, 101, 828 and 3500 ps (Table S7). Notably, at least two of them are on the sub-nanosecond timescale. For a more detailed understanding we turned to target analyses using the model displayed in Figure 5: it includes four different states and considers three parallel branches, which are all born from a vibrationally hot excited state (Table S8). Singlet excited states are nondetectable with our time resolution due to rapid intersystem crossing.[58] As such, the first observable states upon 387 nm photoexcitation should be vibrationally hot ^{3}MLCTs of {Ru(py)$_4$} and {Ru(tpy)(bpy)}. Our model assigns a single excited state precursor, namely **hot-^{3}MLCT**, that accounts for both of them and the differential absorption spectrum is a "mixed" excited state.[59] Within 7 ps, which is characteristic for vibrational cooling,[47,60–64] three well distinguishable excited states are populated. Two of them are ascribed to **^{3}MLCTz** and **^{3}MLCTxy**, since their species associated differential absorption spectra and their lifetimes match those obtained in nanosecond experiments (vide supra).[65] This leaves only the third excited state unassigned. Based on a decay of 110 ps, we hypothesize that it is a remote ^{3}MLCT, in which the electron is on the tpy ligand and the hole is localized in {Ru(py)$_4$}. Important for our assignment are the presence of two typical photoinduced absorptions associated with the tpy$^{\bullet-}$ radical anion at 21050 and 16100 cm^{-1} (475 and 620 nm, respectively) and the stronger bleach at ~390 nm. This **^{3}MLCTr** state, formally described as {Ru^{II}(tpy$^-$)(bpy)(μ-CN)Ru^{III}(py)$_4$Cl}, decays faster than any of the other two states. Most likely thermal population of {Ru(py)$_4$}-based *dd* states is responsible for its short lifetime.[66,67]

Independent confirmation for our model came from picosecond vis-NIR transient absorption measurements with argon-saturated DMSO solutions, but with 505 nm rather than 387 nm illumination (Figure S17). Only {Ru(tpy)(bpy)} is excited and **^{3}MLCTr** is not expected to participate in the overall decay cascade. In fact, target analyses based on a model with only three excited states was sufficient to afford a good fit: **hot-^{3}MLCT**, **^{3}MLCTz**, and **^{3}MLCTxy** (Figures S17 and S18). Figure S19 illustrates the presence of an additional process under 387 nm excitation in comparison with 505 nm excitation.

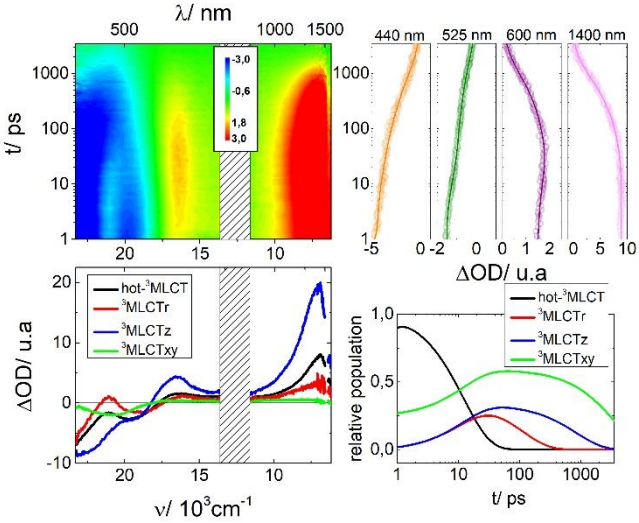

Figure 4. Upper left: Differential absorption 3D map obtained from picosecond pump-probe experiments (λ_{exc}= 387 nm) for [RuRu]$^{2+}$ in DMSO at room temperature. Upper right: Time absorption profiles (open circles) and corresponding fittings from target analysis (solid lines). Bottom left: Species-associated differential spectra of **hot-^{3}MLCT** (black line), **^{3}MLCTr** (red line), **^{3}MLCTz** (blue line) and **^{3}MLCTxy** (green line) for [RuRu]$^{2+}$ upon excitation at 387 nm. Bottom right: concentration evolution over time.

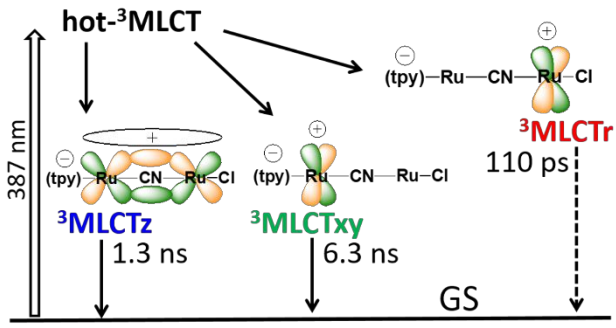

Figure 5. Kinetic model for $[RuRu]^{2+}$ under 387 nm excitation.

The coexistence of **³MLCTz** and **³MLCTxy** brings up questions related to their energy difference and their interconversion. We believe that they are nearly degenerate in terms of energy and it is difficult to unambiguously corroborate if **³MLCTz** or **³MLCTxy** are at a lower energy. On one hand, delocalization is expected to stabilize **³MLCTz** with respect to **³MLCxy**. On the other hand, in both states the excited electron sits in a tpy-based orbital pointing to the d_{xy} metallic orbital, so electron-hole mutual interactions tend to stabilize **³MLCTxy** with respect to **³MLCTz**. Moreover, why are they not interconverting on shorter timescales as it happens in $[Ru(tpm)(bpy)(NCS)]^{+}$?[49,68] The origin of the kinetic barrier, which is responsible for this behaviour, probably relates to the different nature of the orbitals that the holes occupy in the two states. In **³MLCTz**, the positive charge density is distributed over the {RuRu} fragment. Interconversion to **³MLCTxy** would imply a charge redistribution to a single {Ru} and would involve changes in bond distances and angles, as it usually occurs in the decay of ³MLCT excited state to the ground state. Our rationale is consistent with the barrier observed in $[Ru(tpm)(bpy)(NCS)]^{+}$,[49] where a charge redistribution occurs from a {Ru} to a {Ru(NCS)}, involving, however, a smaller number of bond distances and angles than in $[RuRu]^{2+}$. Accordingly, the barrier is smaller in $[Ru(tpm)(bpy)(NCS)]^{+}$ and allows for the interconversion between ³MLCT excited states of different symmetry on a timescale of 300 ps.

CONCLUSION

Here, we demonstrate the use of NIR photoinduced absorptions of bimetallic $[Ru(tpy)(bpy)(\mu\text{-}CN)Ru(py)_4Cl]^{2+}$ ($[RuRu]^{2+}$) to identify the coexistence of two long lived mixed valence excited state. This is of utmost importance for the design of photoactive materials based on coordination compounds as such a configuration enables different reactivity. In a recent contribution,[49] trapping of ³MLCT states of different symmetry was observed in monometallic {Ru(bpy)} complexes. To this end, the current work shows another instance of the presence of two low energy excited states with different electronic configurations. We document the possibility to exert spatial control over the aforementioned states by just adding a second metal centre. In the corresponding $[RuRu]^{2+}$, the net result is that only the wavefunctions of the appropriate symmetry delocalize over the bimetallic fragment, while the wavefunctions, which are mostly orthogonal to the intermetallic axis, remain localized. The observation of this phenomenon paves the way to design functional molecular systems, where excited states of different symmetry are populated. $[Ru(tpy)(bpy)(\mu\text{-}CN)Ru(py)_4(\mu\text{-}NC)Cr(CN)_5]$, for example, is a very interesting case. Energy transfer from the Ru fragments to the Cr fragment is known. It should, however, strongly depend on the symmetry of the populated {RuRu} excited state. We are hopeful to apply our NIR transient absorption diagnostics for the elucidation of the underlying reaction mechanism.

ASSOCIATED CONTENT

Supporting Information

The Supporting Information is available free of charge on the ACS Publications website. The PDF file includes experimental details, (TD)DFT calculations, absorption/excitation/emission spectra, TCSPC measurements, photolysis experiments, selected transient absorption spectra, transient absorption 3D maps, fittings and models.

AUTHOR INFORMATION

Corresponding Authors

*acadranel@qi.fcen.uba.ar
*dirk.guldi@fau.de

ORCID

Paola S. Oviedo: 0000-0002-9643-3884
German E. Pieslinger: 0000-0003-1334-5211
Luis M. Baraldo: 0000-0003-0666-5540
Alejandro Cadranel: 0000-0002-6597-4397
Dirk M. Guldi: 0000-0002-3960-1765

Notes

The authors declare no competing financial interests.

ACKNOWLEDGMENTS

This work was supported by grants from the University of Buenos Aires (UBACyT 20020130100534BA), CONICET (PIP 112-20150100394CO) and ANPCyT (PICT 2013 00069). PSO gratefully acknowledges a doctoral fellowship from CONICET and funding from ANPCyT to visit FAU Erlangen-Nürnberg, and AC a postdoctoral grant from DAAD-ALEARG. GEP thanks Prof. Dr. Adrián Roitberg for selflessly sharing his knowledge and DAAD for personal funding. LMB and AC are members of the research staff of CONICET and GEP is postdoctoral fellow of the same institution. AC thanks ALN for remote assistance.

REFERENCES

(1) Whang, D. R.; Apaydin, D. H. Artificial Photosynthesis: Learning from Nature. *ChemPhotoChem* **2018**, *2* (3), 148–160.

(2) El-Khouly, M. E.; El-Mohsnawy, E.; Fukuzumi, S. Solar Energy Conversion: From Natural to Artificial Photosynthesis. *J. Photochem. Photobiol. C Photochem. Rev.* **2017**, *31*, 36–83.

(3) House, R. L.; Iha, N. Y. M.; Coppo, R. L.; Alibabaei, L.; Sherman, B. D.; Kang, P.; Brennaman, M. K.; Hoertz, P. G.; Meyer, T. J. Artificial Photosynthesis: Where Are We Now? Where Can We Go? *J. Photochem. Photobiol. C Photochem.*

Rev. **2015**, *25*, 32–45.

(4) Balzani, V.; Credi, A.; Venturi, M. *Molecular Devices and Machines– A Journey into the Nano World*; Wiley-VCH Verlag GmbH & Co. KGaA: Weinheim, FRG, 2003.

(5) Kuriki, R.; Yamamoto, M.; Higuchi, K.; Yamamoto, Y.; Akatsuka, M.; Lu, D.; Yagi, S.; Yoshida, T.; Ishitani, O.; Maeda, K. Robust Binding between Carbon Nitride Nanosheets and a Binuclear Ruthenium(II) Complex Enabling Durable, Selective CO 2 Reduction under Visible Light in Aqueous Solution. *Angew. Chemie Int. Ed.* **2017**, *56* (17), 4867–4871.

(6) Concepcion, J. J.; Jurss, J. W.; Hoertz, P. G.; Meyer, T. J. Catalytic and Surface-Electrocatalytic Water Oxidation by Redox Mediator-Catalyst Assemblies. *Angew. Chem. Int. Ed. Engl.* **2009**, *48* (50), 9473–9476.

(7) Braumüller, M.; Schulz, M.; Sorsche, D.; Pfeffer, M.; Schaub, M.; Popp, J.; Park, B.-W.; Hagfeldt, A.; Dietzek, B.; Rau, S. Synthesis and Characterization of an Immobilizable Photochemical Molecular Device for H 2 -Generation. *Dalt. Trans.* **2015**, *44* (12), 5577–5586.

(8) Gholamkhass, B.; Koike, K.; Negishi, N.; Hori, H.; Sano, T.; Takeuchi, K. Adjacent- versus Remote-Site Electron Injection in TiO 2 Surfaces Modified with Binuclear Ruthenium Complexes. *Inorg. Chem.* **2003**, *42* (9), 2919–2932.

(9) Cerfontaine, S.; Marcélis, L.; Laramee-Milette, B.; Hanan, G. S.; Loiseau, F.; De Winter, J.; Gerbaux, P.; Elias, B. Converging Energy Transfer in Polynuclear Ru(II) Multiterpyridine Complexes: Significant Enhancement of Luminescent Properties. *Inorg. Chem.* **2018**, *57* (5), 2639–2653.

(10) Balzani, V.; Bergamini, G.; Campagna, S.; Puntoriero, F. Photochemistry and Photophysics of Coordination Compounds: Overview and General Concepts. In *Photochemistry and Photophysics of Coordination Compounds I*; Balzani, V and Campagna, S., Ed.; Springer Berlin Heidelberg: Berlin, Heidelberg, 2007; Vol. 280, pp 1–36.

(11) Argazzi, R.; Murakami Iha, N. Y.; Zabri, H.; Odobel, F.; Bignozzi, C. A. Design of Molecular Dyes for Application in Photoelectrochemical and Electrochromic Devices Based on Nanocrystalline Metal Oxide Semiconductors. *Coord. Chem. Rev.* **2004**, *248* (13–14), 1299–1316.

(12) Bignozzi, C. A.; Argazzi, R.; Garcia, C. G.; Scandola, F.; Schoonover, J. R.; Meyer, T. J. Long-Range Energy Transfer in Oligomeric Metal Complex Assemblies. *J. Am. Chem. Soc.* **1992**, *114* (22), 8727–8729.

(13) Ashford, D. L.; Gish, M. K.; Vannucci, A. K.; Brennaman, M. K.; Templeton, J. L.; Papanikolas, J. M.; Meyer, T. J. Molecular Chromophore-Catalyst Assemblies for Solar Fuel Applications. *Chem. Rev.* **2015**, *115* (23), 13006–13049.

(14) De Cola, L. Photoinduced Energy and Electron Transfer Processes in Rigidly Bridged Dinuclear Ru/Os Complexes. *Coord. Chem. Rev.* **1998**, *177* (1), 301–346.

(15) Kleverlaan, C.; Alebbi, M.; Argazzi, R.; Bignozzi, C. A.; Hasselmann, G. M.; Meyer, G. J. Molecular Rectification by a Bimetallic Ru–Os Compound Anchored to Nanocrystalline TiO 2. *Inorg. Chem.* **2000**, *39* (7), 1342–1343.

(16) Mondal, S.; Das, T.; Maity, A.; Seth, S. K.; Purkayastha, P. Synergic Influence of Reverse Micelle Confinement on the Enhancement in Photoinduced Electron Transfer to and from Carbon Nanoparticles. *J. Phys. Chem. C* **2015**, *119* (24), 13887–13892.

(17) Ji, X.; Wang, J.; Mei, L.; Tao, W.; Barrett, A.; Su, Z.; Wang, S.; Ma, G.; Shi, J.; Zhang, S. Porphyrin/SiO 2 /Cp*Rh(Bpy)Cl Hybrid Nanoparticles Mimicking Chloroplast with Enhanced Electronic Energy Transfer for Biocatalyzed Artificial Photosynthesis. *Adv. Funct. Mater.* **2018**, *28* (9), 1705083.

(18) Rogers, H. M.; Arachchige, S. M.; Brewer, K. J. Enhancement of Solar Fuel Production Schemes by Using a Ru,Rh,Ru Supramolecular Photocatalyst Containing Hydroxide Labile Ligands. *Chem. - A Eur. J.* **2015**, *21* (47), 16948–16954.

(19) Erdmann, E.; Lütgens, M.; Lochbrunner, S.; Seidel, W. W. Ultrafast Energy Transfer in Dinuclear Complexes with Bridging 1,10-Phenanthroline-5,6-Dithiolate. *Inorg. Chem.* **2018**, *57* (9), 4849–4863.

(20) Schönweiz, S.; Rommel, S. A.; Kübel, J.; Micheel, M.; Dietzek, B.; Rau, S.; Streb, C. Covalent Photosensitizer-Polyoxometalate-Catalyst Dyads for Visible-Light-Driven Hydrogen Evolution. *Chem. - A Eur. J.* **2016**, *22* (34), 12002–12005.

(21) Demadis, K. D.; Hartshorn, C. M.; Meyer, T. J. The Localized-to-Delocalized Transition in Mixed-Valence Chemistry. *Chem. Rev.* **2001**, *101* (9), 2655–2686.

(22) *Mixed Valency Systems: Applications in Chemistry, Physics and Biology*; Prassides, K., Ed.; Springer Netherlands: Dordrecht, 1991.

(23) Glover, S. D.; Goeltz, J. C.; Lear, B. J.; Kubiak, C. P. Mixed Valency at the Nearly Delocalized Limit: Fundamentals and Forecast. *Eur. J. Inorg. Chem.* **2009**, *2009* (5), 585–594.

(24) Kaim, W.; Lahiri, G. K. Unconventional Mixed-Valent Complexes of Ruthenium and Osmium. *Angew. Chemie Int. Ed.* **2007**, *46* (11), 1778–1796.

(25) Launay, J.-P. Long-Distance Intervalence Electron Transfer. *Chem. Soc. Rev.* **2001**, *30* (6), 386–397.

(26) Murase, R.; Leong, C. F.; D'Alessandro, D. M. Mixed Valency as a Strategy for Achieving Charge Delocalization in Semiconducting and Conducting Framework Materials. *Inorg. Chem.* **2017**, *56* (23), 14373–14382.

(27) Creutz, C.; Taube, H. Direct Approach to Measuring the Franck-Condon Barrier to Electron Transfer between Metal Ions. *J. Am. Chem. Soc.* **1969**, *91* (14), 3988–3989.

(28) Creutz, C. Mixed Valence Complexes of D5-D6 Metal Centers. In *Progress in Inorganic Chemistry*; John Wiley & Sons, Inc., 1983; pp 1–73.

(29) D'Alessandro, D. M.; Keene, F. R. Current Trends and Future Challenges in the Experimental, Theoretical and Computational Analysis of Intervalence Charge Transfer (IVCT) Transitions. *Chem. Soc. Rev.* **2006**, *35* (5), 424–440.

(30) D'Alessandro, D. M.; Keene, F. R. Intervalence Charge Transfer (IVCT) in Trinuclear and Tetranuclear Complexes of Iron, Ruthenium, and Osmium. *Chem. Rev.* **2006**, *106* (6), 2270–2298.

(31) Matsui, K.; Nazeeruddin, M. K.; Humphry-Baker, R.; Grätzel, M.; Kalyanasundaram, K. Transient Absorptions Due to Mixed Valence Species in the Excited State Absorption Spectra of Cyano-Bridged Trinuclear Polypyridyl Complexes of Ruthenium(II). *J. Phys. Chem.* **1992**, *96* (26), 10587–10590.

(32) Bignozzi, C. A.; Argazzi, R.; Chiorboli, C.; Scandola, F.; Dyer, R. B.; Schoonover, J. R.; Meyer, T. J. Vibrational and Electronic Spectroscopy of Electronically Excited Polychromophoric Ruthenium(II) Complexes. *Inorg. Chem.* **1994**, *33* (8), 1652–1659.

(33) Bignozzi, C. A.; Indelli, M. T.; Scandola, F. Bis(2,2'-Bipyridine)Ruthenium(II)-Hexacyanochromate(III) Chromophore-Luminophore Complexes. Intramolecular Energy Transfer, Excited-State Intervalence Transfer, and Doublet-Doublet Annihilation. *J. Am. Chem. Soc.* **1989**, *111* (14), 5192–5198.

(34) Indelli, M. T.; Scandola, F. Excited-State Charge Recombination in a Ruthenium(II)-Chromium(III) Polynuclear Complex. *J. Phys. Chem.* **1993**, *97* (13), 3328–3332.

(35) Fleming, C. N.; Dattelbaum, D. M.; Thompson, D. W.; Ershov, A. Y.; Meyer, T. J. Excited State Intervalence Transfer in a Rigid Polymeric Film. *J. Am. Chem. Soc.* **2007**, *129* (31),

9622–9630.

(36) Lambert, C.; Wagener, R.; Klein, J. H.; Grelaud, G.; Moos, M.; Schmiedel, A.; Holzapfel, M.; Bruhn, T. A Photoinduced Mixed-Valence State in an Organic Bis-Triarylamine Mixed-Valence Compound with an Iridium-Metal-Bridge. *Chem. Commun.* **2014**, *50* (77), 11350.

(37) Henderson, J.; Kubiak, C. P. Photoinduced Mixed Valency in Zinc Porphyrin Dimer of Triruthenium Cluster Dyads. *Inorg. Chem.* **2014**, *53* (20), 11298–11306.

(38) Henderson, J.; Glover, S. D.; Lear, B. J.; Walker, D.; Winkler, J. R.; Gray, H. B.; Kubiak, C. P. Electron-Transfer Reactions of Electronically Excited Zinc Tetraphenylporphyrin with Multinuclear Ruthenium Complexes. *J. Phys. Chem. B* **2015**, *119* (24), 7473–7479.

(39) Dattelbaum, D. M.; Hartshorn, C. M.; Meyer, T. J. Direct Measurement of Excited-State Intervalence Transfer in [(Tpy)Ru III (Tppz •-)Ru II (Tpy)] 4+ * by Time-Resolved Near-Infrared Spectroscopy. *J. Am. Chem. Soc.* **2002**, *124* (18), 4938–4939.

(40) Kalyanasundaram, K.; Nazeeruddin, M. K. Inter-Chromophore Electronic Interactions in Ligand-Bridged Polynuclear Complexes: A Comparative Study of Various Bridging Ligands. *Inorganica Chim. Acta* **1994**, *226* (1–2), 213–230.

(41) Cadranel, A.; Tate, J. E.; Oviedo, P. S.; Yamazaki, S.; Hodak, J. H.; Baraldo, L. M.; Kleiman, V. D. Distant Ultrafast Energy Transfer in a Trimetallic {Ru–Ru–Cr} Complex Facilitated by Hole Delocalization. *Phys. Chem. Chem. Phys.* **2017**, *19* (4), 2882–2893.

(42) Jude, H.; Rein, F. N.; White, P. S.; Dattelbaum, D. M.; Rocha, R. C. Synthesis, Structure, and Electronic Properties of a Dimer of Ru(Bpy) 2 Doubly Bridged by Methoxide and Pyrazolate. *Inorg. Chem.* **2008**, *47* (17), 7695–7702.

(43) Oviedo, P. S.; Pieslinger, G. E.; Cadranel, A.; Baraldo, L. M. Exploring the Localized to Delocalized Transition in Non-Symmetric Bimetallic Ruthenium Polypyridines. *Dalt. Trans.* **2017**, *46* (45), 15757–15768.

(44) Juris, A.; Balzani, V.; Barigelletti, F.; Campagna, S.; Belser, P.; von Zelewsky, A. Ru(II) Polypyridine Complexes: Photophysics, Photochemistry, Eletrochemistry, and Chemiluminescence. *Coord. Chem. Rev.* **1988**, *84* (C), 85–277.

(45) Given the low photoluminescence quantum yields of $[RuRu]^{2+}$, a typical TCSPC experiment takes up to four hours. During such a long period of irradiation, photodecomposition of $[RuRu]^{2+}$ sets in. We ascribe the third, longest exponential component to photoluminescence from photoproducts. Such a long-lived component was not detected in 15-minutes-long transient absorption experiments. Photolysis experiments reveal photodecomposition quantum yields far below 1% (Figure S6).

(46) All attempts to include an additional longer component consistent with the TCSPC results failed.

(47) Rachford, A. A.; Rack, J. J. Picosecond Isomerization in Photochromic Ruthenium–Dimethyl Sulfoxide Complexes. *J. Am. Chem. Soc.* **2006**, *128* (44), 14318–14324.

(48) Rasmussen, S. C.; Ronco, S. E.; Mlsna, D. A.; Billadeau, M. A.; Pennington, W. T.; Kolis, J. W.; Petersen, J. D. Ground- and Excited-State Properties of Ruthenium(II) Complexes Containing Tridentate Azine Ligands, Ru(Tpy)(Bpy)L2+, Where L Is a Polymerizable Acetylene. *Inorg. Chem.* **1995**, *34* (4), 821–829.

(49) Cadranel, A.; Oviedo, P. S.; Pieslinger, G. E.; Yamazaki, S.; Kleiman, V. D.; Baraldo, L. M.; Guldi, D. M. Trapping Intermediate MLCT States in Low-Symmetry {Ru(Bpy)} Complexes. *Chem. Sci.* **2017**, *8* (11), 7434–7442.

(50) Cohen, A. J.; Mori-Sanchez, P.; Yang, W. Insights into Current Limitations of Density Functional Theory. *Science* **2008**, *321* (5890), 792–794.

(51) Vydrov, O. A.; Scuseria, G. E.; Perdew, J. P. Tests of Functionals for Systems with Fractional Electron Number. *J. Chem. Phys.* **2007**, *126* (15), 154109.

(52) Zhang, Y.; Yang, W. A Challenge for Density Functionals: Self-Interaction Error Increases for Systems with a Noninteger Number of Electrons. *J. Chem. Phys.* **1998**, *109* (7), 2604–2608.

(53) Perdew, J. P.; Levy, M. Comment on "Significance of the Highest Occupied Kohn-Sham Eigenvalue." *Phys. Rev. B* **1997**, *56* (24), 16021–16028.

(54) Robin, M. B.; Day, P. Mixed Valence Chemistry-A Survey and Classification. In *Advances in Inorganic Chemistry and Radiochemistry*; 1968; Vol. 10, pp 247–422.

(55) Alborés, P.; Slep, L. D.; Weyhermüller, T.; Baraldo, L. M. Fine Tuning of the Electronic Coupling between Metal Centers in Cyano-Bridged Mixed-Valent Trinuclear Complexes. *Inorg. Chem.* **2004**, *43* (21), 6762–6773.

(56) Alborés, P.; Rossi, M. B.; Baraldo, L. M.; Slep, L. D. Donor–Acceptor Interactions and Electron Transfer in Cyano-Bridged Trinuclear Compounds. *Inorg. Chem.* **2006**, *45* (26), 10595–10604.

(57) Pieslinger, G. E.; Aramburu-Trošelj, B. M.; Cadranel, A.; Baraldo, L. M. Influence of the Electronic Configuration in the Properties of d 6 –d 5 Mixed-Valence Complexes. *Inorg. Chem.* **2014**, *53* (16), 8221–8229.

(58) McCusker, J. K. Femtosecond Absorption Spectroscopy of Transition Metal Charge-Transfer Complexes. *Acc. Chem. Res.* **2003**, *36* (12), 876–887.

(59) All Our Attempts to Deconvolute the Initially Populated Ex-Cited State Failed.

(60) Damrauer, N. H.; McCusker, J. K. Ultrafast Dynamics in the Metal-to-Ligand Charge Transfer Excited-State Evolution of [Ru(4,4'-Diphenyl-2,2'-Bipyridine) 3] 2+. *J. Phys. Chem. A* **1999**, *103* (42), 8440–8446.

(61) Liu, Y.; Turner, D. B.; Singh, T. N.; M, A.; Chouai, A.; Dunbar, K. R.; Turro, C. Ultrafast Ligand Exchange : Detection of a Pentacoordinate Ru (II) Intermediate and Product Formation Ultrafast Ligand Exchange : Detection of a Pentacoordinate Ru (II) Intermediate. *J. Am. Chem. Soc.* **2009**, *131* (Ii), 26–27.

(62) McFarland, S. A.; Lee, F. S.; Cheng, K. A. W. Y.; Cozens, F. L.; Schepp, N. P. Picosecond Dynamics of Nonthermalized Excited States in Tris(2,2-Bipyridine)Ruthenium(II) Derivatives Elucidated by High Energy Excitation. *J. Am. Chem. Soc.* **2005**, *127* (19), 7065–7070.

(63) Ramakrishna, G.; Jose, D. A.; Kumar, D. K.; Das, A.; Palit, D. K.; Ghosh, H. N. Ultrafast Dynamics and Excited State Deactivation of [Ru(Bpy) 2 Sq] + and Its Derivatives. *J. Phys. Chem. B* **2006**, *110* (20), 10197–10203.

(64) Bhasikuttan, A. C.; Suzuki, M.; Nakashima, S.; Okada, T. Ultrafast Fluorescence Detection in Tris (2 , 2 ′ -Bipyridine) Ruthenium (II) Complex in Solution : Relaxation Dynamics Involving Higher Excited States. *J. Am. Chem. Soc.* **2002**, *124* (Ii), 8398–8405.

(65) It is worth to mention the limited accuracy of the 3500 ps lifetime extracted from picosecond transient absorption measurements, due to our delay line length of about 5 – 7 ns.

(66) *dd* states are hard to detect because they usually decay faster than they are populated, impeding an observable build-up.

(67) Trace impurities of monomeric {Ru(tpy)(bpy)} complexes could also be responsible for the **^{3}MLCTxy** state in the deactivation cascades of $[RuRu]^{2+}$. These impurities may come from inefficient purification of the samples. Considering our preparation methods, $[Ru(tpy)(bpy)Cl]^+$ and $[Ru(tpy)(bpy)CN]^+$ are reasonable synthetic impurities. However, their MLCT maxima at 500 or 490 nm and their lifetimes in DMSO of 20 and 16 ns for the chlorido and cyanido-complex, respectively, are inconsistent with **^{3}MLCTxy** (475 nm, 6.3 ns). Impurities might also be due to decomposition upon laser illumination: $[Ru(tpy)(bpy)(DMSO)]^+$ may originate from the photolysis of the oligomers and subsequent solvent substitution in {Ru(tpy)(bpy)}.

The ^{3}MLCT characteristics of the oxygen-bound DMSO-complex (475 nm, 8 ns)[47] seem compatible with our results. Nevertheless, **^{3}MLCTxy** is rather insensitive to the solvent. Very similar **^{3}MLCTxy** states are observed in transient absorption experiments with $[RuRu]^{2+}$ performed in water (470 nm, 3.9 ns) or ACN (480 nm, 3.4 ns) (Figure S15). These are, in turn, inconsistent with the MLCT excited states observed for $[Ru(tpy)(bpy)(OH_2)]^{2+}$ in water (480 nm, 200 ps),[69] and $[Ru(tpy)(bpy)(ACN)]^{2+}$ in ACN (no bleach, 450 ps, Figure S16). Therefore, the formation of a solvento-complex via photolysis in transient absorption experiments can be safely ruled out.)

(68) Internal conversion between these states may set in, but on a timescale comparable to their lifetimes. The lifetime of **^{3}MLCTxy** is shorter than that of MLCT states in $[Ru(tpy)(bpy)(CN)]^+$. A **^{3}MLCTxy** to **^{3}MLCTz** internal conversion might be responsible for this. In the monometallic reference, monoexponential fittings render only one time constant of 13.4 ns upon 505 nm excitation and 12.2 ns upon 387 nm excitation in DMSO. Nevertheless, the lack of PILMCT (as in {Ru(NCS)} complexes)[49] or PIIVCT spectroscopic markers hampers unequivocal conclusions about the participation of excited sates of different symmetries in the deactivation cascades. Analogously, a **^{3}MLCTz** to **^{3}MLCTxy** process might shorten the lifetime of **^{3}MLCTz** in comparison to typical ^{3}MLCT states. In this case, however, the delocalized nature might favour interactions with $\{Ru(py)_4\}$-centred *dd* states, which could also contribute as a deactivation pathway.

(69) Hewitt, J. T.; Concepcion, J. J.; Damrauer, N. H. Inverse Kinetic Isotope Effect in the Excited-State Relaxation of a Ru(II)–Aquo Complex: Revealing the Impact of Hydrogen-Bond Dynamics on Nonradiative Decay. *J. Am. Chem. Soc.* **2013**, *135* (34), 12500–12503.

TOC graphic

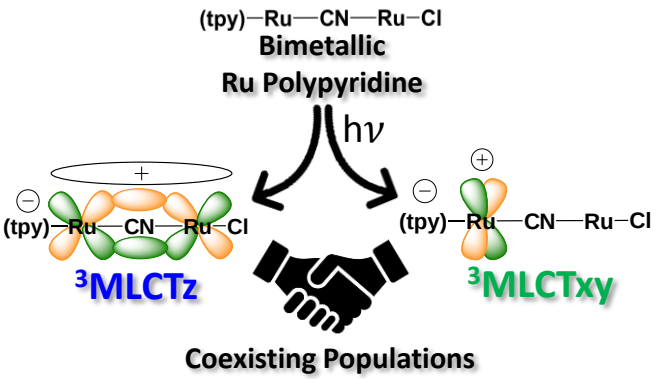

Synopsis

Photoexcitation of $[Ru(tpy)(bpy)(\mu\text{-}CN)Ru(py)_4Cl]^{2+}$ results in the simultaneous population of two ^{3}MLCT excited states of different symmetry. In **^{3}MLCTz** the hole sits in an orbital parallel to the intermetallic axis allowing for a strong metal-metal electronic coupling and intense photoinduced intervalence charge transfer (PIIVCT) NIR absorptions. In **^{3}MLCTxy** the hole is localized in an orbital perpendicular to the intermetallic axis and, in turn, significant intermetallic coupling is absent.